Chapter 12
Microwave Absorption Behaviour

The high-frequency absorption behaviour of amorphous ferromagnetic materials, among others, is of considerable interest for microwave absorber applications [1]. Since amorphous glass-coated microwires have small dimensions (1–30 μm in diameter), high electrical conductivity ($\sim 6\times10^5$ S/m), high magnetic permeability ($\sim 10^4$), and high mechanical strength ($\sim 10^3$ MPa), they can be incorporated into polymer-based composites for creating high-performance microwave absorption [2–4] or EMI shielding [5] composite materials. Compared with dielectric absorbents, magnetic absorbents provide additional magnetic losses and achieve a better impedance match. Compared to other types of magnetic absorbent, e.g. the widely used ferrites, the soft magnetic materials are not as limited by Snoek's law thanks to their large saturation magnetisation and permeability. But their issue lies in the large conductivity, which could make them useless for high-frequency applications owing to the strong eddy current loss, which is formulated as [6]:

$$P_e = \frac{CB^2f^2d^2}{\rho}, \tag{12.1}$$

where C is the proportional constant, B is the flux density, f is the frequency, d is the sample thickness and ρ is the resistivity. In a composite material, the concentration p has to be considered, and Eq. (12.1) can then be revised to [7] the following:

$$P_e = p\frac{CB^2f^2d^2}{\rho}. \tag{12.2}$$

For the low-resistivity material to be used in high frequency, the immediate approach to curb the eddy current loss as indicated by Eq. (12.2) is to limit the thickness of the absorbent (wire diameter in the case of microwire-based absorber) or its concentration in the composite absorber. This is de facto one of the basic rationales for our adopting thin ferromagnetic microwires of limited concentration for microwave absorption at gigahertz, and more relevant details will be discussed later. Another distinct advantage is that microwire composites possess remarkable tunable properties, as presented in the last chapter, rendering likely a broader absorption band compared to their non-tunable counter parts [8].

H.-X. Peng et al., *Ferromagnetic Microwire Composites*,
Engineering Materials and Processes, DOI 10.1007/978-3-319-29276-2_12

In view of the appealing application potential of microwire absorbents, the former Soviet Union had expended enormous efforts investigating the microwave absorption properties of amorphous microwires, but few results are available to the public for confidentiality reasons. Not until 2009 did the Micromag company of Spain successfully commercialise amorphous microwires as absorbents in warships.

A number of groups worldwide have been actively engaged in the development of microwire-based absorbers and shielders, and their seminal works will be surveyed below. It is also worth mentioning that, although microwire composites also exhibit excellent shielding properties in both a regular [5] and a random manner [9], the EMI shielding is absorption-dominated [5, 10]. We will therefore focus on the discussion of the microwave absorption of microwire composites, which is determined by their electromagnetic constitutive parameters, namely permittivity and permeability, through the intrinsic properties of microwires and their mesostructure. The rest of this chapter is organised as follows. A brief introduction to microwave absorption theory will first be given. Two types of microwire absorber will be treated separately, according to the absorption mechanism, i.e. dielectric loss dominated and magnetic loss dominated absorbers. Finally, the design strategies of some specific absorbers containing microwire-based fillers are described.

12.1 Microwave Absorption Theory

While the phenomenon of microwave absorption (MA) has been known for many decades and the cause of the absorption is well formulated, the design of absorbers has occupied the minds of many materials scientists and engineers for centuries. Recently, the problem has garnered even more attention and become more important than ever. In addition to academic reasons, its practical impact on society has been recognised. The growing public concern about possible human health effects in relation to weak RF fields, i.e. health hazards from environmental fields [11], motivates the related research.

In this section, fundamental knowledge of microwave absorption will be presented as well as an overview of mixture law theory. These two together provide a theoretical route to an optimised design of absorbers. Microwave energy, when incident on a lossy dispersive material, creates heating within the material through the interactions of the electromagnetic field with the materials' molecular and electronic structure. Homogeneous and heterogeneous media analysed with in an effective medium approach are described by two material parameters: the complex (relative) permittivity $\varepsilon = \varepsilon' - j\varepsilon''$ and the magnetic permeability (relative) $\mu = \mu' - j\mu''$. The terms ε' and μ' are associated with energy storage, and terms ε'' and μ'' are associated with dielectric loss or energy dissipation within a material, resulting from conduction, resonance, and relaxation mechanisms. The loss tangent of the dielectric material is $\tan\delta = \varepsilon''/\varepsilon'$, where δ is the dielectric loss angle of the material. Energy loss in a material illuminated by electromagnetic waves comes about through damping forces acting on polarised atoms and molecules and through

the finite conductivity of a material. It is common knowledge in electromagnetism that the Poynting theorem governs our understanding of the conservation of power in linear, dispersive media [12]. This states that the total power (for a harmonic electromagnetic field of angular frequency ω entering a volume V through the surface S) goes partially into increasing the field energy stored inside V and is partially lost into heat, i.e.

$$\frac{\partial u}{\partial t} + \nabla \cdot S = -j \cdot E - 2\omega Im\left(\varepsilon\left\langle |E|^2 \right\rangle + \mu\left\langle |H|^2 \right\rangle\right), \tag{12.3}$$

where

$$u = \mathrm{Re}\left[\varepsilon_0 \frac{\mathrm{d}(\omega\varepsilon)}{\mathrm{d}\omega}\left\langle |E|^2 \right\rangle + \mu_0 \frac{\mathrm{d}(\omega\mu)}{\mathrm{d}\omega}\left\langle |H|^2 \right\rangle\right], \tag{12.4}$$

where $\langle \ldots \rangle$ denotes the time average over the period of the carrier frequency, and $S = E \times H$ is the Poynting vector. The quantities ε_0 and μ_0 are the permittivity and the magnetic permeability of vacuum, respectively. The quantities E and H are the electric and magnetic field intensities, respectively. The quantity j accounts for both conductive and dielectric losses. We observe that the conductive and dielectric losses are indistinguishable with respect to the heat generated. Applying external electromagnetic fields to a composite material implies that the electromagnetic waves come across a variety of microscopic boundary conditions due to the inclusions making the heterostructure. The resulting local field variations can have a very strong effect on energy absorption at such boundaries, since absorption depends quadratically on the electric field intensity.

Figure 12.1 shows a multilayer microwave absorber which consists of n layers of different materials backed by a perfect electric conductor (PEC). For simplicity, we consider that the electromagnetic wave is normally incident. Here, d_i, μ_i and ε_i denote the thickness, the complex intrinsic impedance, and the propagation constant of the ith layer, respectively. The conductivity for each individual layer of the

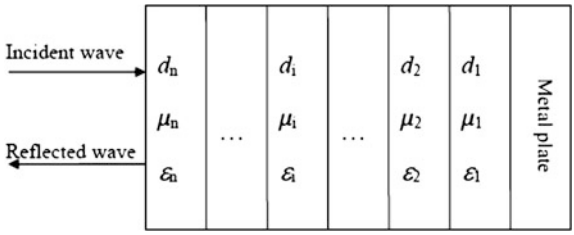

Fig. 12.1 Schematic of a multilayer microwave absorber with a normally incident wave. d_i, μ_i, and ε_i denote the thickness, relative permeability, and permittivity of the ith layer, respectively

absorber is assumed to be zero. According to the transmission-line theory [13–15], the wave impedance (Z_i) of the ith layer is given by

$$Z_i = \eta_i \frac{Z_{i-1} + \eta_i \tan h(\gamma_i d_i)}{\eta_i + Z_{i-1} \tan h(\gamma_i d_i)}, \tag{12.5}$$

where $\eta_i = \eta_0 \sqrt{\mu_i / \varepsilon_i}$, $\gamma_i = j2\pi f \sqrt{\mu\varepsilon}/c$, η_0 are the characteristic impedance of the free space; μ_i and ε_i are the relative complex permeability and permittivity of the ith layer, respectively. Considering that the metal plate is a PEC, $\eta_0 = 0$, the impedance of first layer reads as follows:

$$Z_1 = \eta_1 \tan h(\gamma_1 d_1). \tag{12.6}$$

The reflection loss (RL) of the normal incident electromagnetic wave at the absorber surface is given by

$$\mathrm{RL} = 20 \log|\Gamma| = 20 \log \left| \frac{Z_n - \eta_0}{Z_n + \eta_0} \right|, \tag{12.7}$$

where Γ is the reflection coefficient. Through Eqs. (12.5)–(12.7), we can see that the combination of the magnetic permeability and the permittivity (of both the absorbing and the substrate layers) satisfying the impedance matching condition is the key to producing a high-performance microwave absorber. Specifically, for a single layer of absorber backed by a PEC, which is a common situation in many studies discussed above, the reflection loss is given as follows:

$$\mathrm{RL} = 20 \log \left| \frac{\sqrt{\frac{\mu}{\varepsilon}} \tan h\left(j \frac{2\pi f d}{c} \sqrt{\mu\varepsilon}\right) - 1}{\sqrt{\frac{\mu}{\varepsilon}} \tan h\left(j \frac{2\pi f d}{c} \sqrt{\mu\varepsilon}\right) + 1} \right|. \tag{12.8}$$

The attenuation constant α (real part of the propagation factor γ), in nepers/m, is defined by [13]:

$$\begin{aligned} \alpha &= \mathrm{Re}(\gamma) \\ &= \mathrm{Re}\left(\frac{j\omega\sqrt{\mu\varepsilon}}{c} \right) \\ &= \frac{\omega}{\sqrt{2}c} \sqrt{\mu''\varepsilon'' - \mu'\varepsilon' + \sqrt{(\mu'^2 + \mu''^2)(\varepsilon'^2 + \varepsilon''^2)}}. \end{aligned} \tag{12.9}$$

where c is the light speed in free space. Here we can see that the attenuation constant is dependent on complex magnetic permeability, permittivity, and frequency. If we consider diamagnetic carbonaceous materials, MA is due to dielectric losses. Before we proceed to consider the case of pure dielectrics with $\mu = 1 - j0$, we first consider for the purpose of comparison the case of ferrites with strong magnetic losses, their absorption being mainly due to the ferromagnetic resonance.

To satisfy the minimum reflection loss, according to Eq. (12.8) the perfect matching condition is given as follows:

$$\sqrt{\frac{\mu}{\varepsilon}}\tan h\left(j\frac{2\pi fd}{c}\sqrt{\mu\varepsilon}\right)=1. \tag{12.10}$$

Usually, $\frac{2\pi fd}{c}\sqrt{\mu\varepsilon}\ll 1$, as the thickness d is much smaller than wavelength and ε is also small. It follows from Eq. (12.10) that

$$j\frac{2\pi fd}{c}(\mu'-j\mu'')=1, \tag{12.11}$$

which can be reduced to

$$\mu'=0 \quad \text{and} \quad \mu''=\frac{c}{2\pi fd}. \tag{12.12}$$

We find that the matching frequency f_{m} is given as:

$$f_{\mathrm{m}}=\frac{c}{2\pi fd\mu''}. \tag{12.13}$$

The matching frequency should generally be the same as the natural resonance frequency, which can be given by [16–18]

$$f=\frac{r}{2\pi}H_a, \tag{12.14}$$

where $\gamma/2\pi=2.8$ MHz/Oe is the gyromagnetic ratio. The anisotropy field H_{a} is given by

$$H_{\mathrm{a}}=\frac{2|K_1|}{\mu_0 M_{\mathrm{s}}}, \tag{12.15}$$

where K_1 is the anisotropy constant and M_s is the saturation magnetisation. A larger saturation magnetisation or smaller anisotropy field will redshift the resonance frequency, which also means an improved absorption bandwidth, since there is a trade-off between the resonance frequency and the absorption bandwidth [19]. We now turn to the case of a dielectric absorbent. Assuming that $\mu=1-j0$, Eq. (12.8) can be written as follows:

$$\mathrm{RL}=20\log\left|\frac{\sqrt{\frac{1}{\varepsilon}}\tan h\left(j\frac{2\pi fd}{c}\sqrt{\varepsilon}\right)-1}{\sqrt{\frac{1}{\varepsilon}}\tan h\left(j\frac{2\pi fd}{c}\sqrt{\varepsilon}\right)+1}\right|. \tag{12.16}$$

As $\sqrt{\frac{1}{\varepsilon}}\tan h\left(j\frac{2\pi fd}{c}\sqrt{\varepsilon}\right)<1$, the best possible matching, i.e. $\sqrt{\frac{1}{\varepsilon}}\tan h\left(j\frac{2\pi fd}{c}\sqrt{\varepsilon}\right)$, achieves maximum. As $\frac{2\pi fd}{c}\sqrt{\mu\varepsilon}\ll 1$, the best possible matching condition is given as follows:

$$\sqrt{\frac{1}{\varepsilon}}=j\frac{2\pi fd}{c}\sqrt{\varepsilon}, \tag{12.17}$$

This can be reduced to

$$\varepsilon'=0,\quad \varepsilon''=\frac{c}{2\pi fd}. \tag{12.18}$$

This is quite similar to Eq. (12.12). At the best matching condition, we can calculate the maximum reflection loss as follows:

$$[RL]_{\max}=20\log\left|\frac{\frac{1}{\varepsilon}-1}{\frac{1}{\varepsilon}+1}\right|. \tag{12.19}$$

After some transformation, we obtain the following:

$$[\mathrm{RL}]_{\max}=20\log\left(1-\frac{4}{2+\varepsilon''(\tan\delta+\frac{1}{\tan\delta})}\right). \tag{12.20}$$

Note that $\tan\delta+\frac{1}{\tan\delta}$ is monotonically decreasing, $\forall\tan\delta<1$. Thus, the maximum reflection loss should be evaluated by considering both ε'' and the loss tangent. The usual case is that larger ε'' gives rise to larger loss tangents, so an optimised ε'' and associated loss tangent can be expected to achieve the maximum absorption condition, (too small or too large ε'' will not favour absorption), as shown in Fig. 12.2. This is further confirmed by the attenuation constant

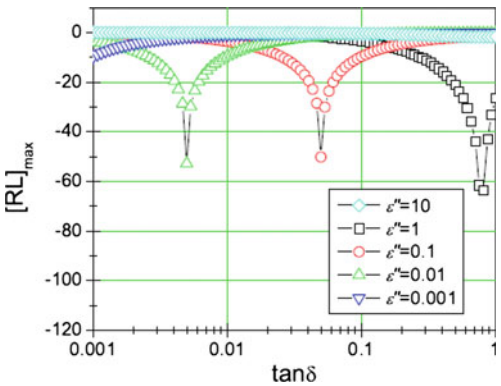

Fig. 12.2 Dielectric loss dependence of the maximum reflection loss for different values of ε''

$$\alpha = \frac{\omega}{\sqrt{2}c}\sqrt{-\varepsilon' + \sqrt{(\varepsilon'^2 + \varepsilon''^2)}}. \tag{12.21}$$

After some transformation, we obtain

$$\alpha = \frac{\omega}{\sqrt{2}c}\sqrt{\varepsilon''\left(\sqrt{1 + \frac{1}{\tan^2\delta}} - \frac{1}{\tan\delta}\right)}. \tag{12.22}$$

At the matching frequency, the attenuation constant reads as follows:

$$\alpha = \frac{\omega}{\sqrt{2}d}\sqrt{\frac{1}{\varepsilon''}\left(\sqrt{1 + \frac{1}{\tan^2\delta}} - \frac{1}{\tan\delta}\right)}. \tag{12.23}$$

12.2 Dielectric Loss Dominated Absorption

In the case of dilute composites, the microwire composites exhibit high complex permittivity but a close-to-unity permeability, with negligible magnetic loss at gigahertz frequency [2, 20, 21]. It follows that the absorption feature is mainly determined by the relaxation polarisation.

The concentration of the wire amount plays an important role in this case. It has been shown that an increasing amount of wires will improve the absorption [5]. However, it is reported that, rather than a simple linear dependence of absorption on the filler content, there is a threshold value at which the percolation network is formed if the glass coatings at the end of wires are spalled, which is often the case [2] (see Fig. 12.3a). This is common in the percolating composite systems (see, e.g. [22–24]). In detail, when the wire content is smaller than the percolation threshold, the loss tangent increases but without a significant increase of dielectric loss as the wire content is increased, whereas further increase of the wire concentration gives a sharp increase of dielectric loss due to the wave reflection rather than absorption. This effect overshadows the contribution of increasing loss tangent to the microwave absorption and results in the decrease of microwave absorption. Note that the tunnelling effect is responsible for the conductivity of the composite before the percolating threshold, which is highly desirable for microwave absorption. It should be mentioned that, at this point, microwires are not as good as ferrite due to its much higher conductivity, which would otherwise free our concerns on the concentration limitation to preserve the dipole nature [25]. To address the conflict between the increasing wire concentration and the percolating network, superior glass quality is the key. Therefore, it is now clear to us that, in addition to the quality of the metallic core, good glass quality is necessary for further improving

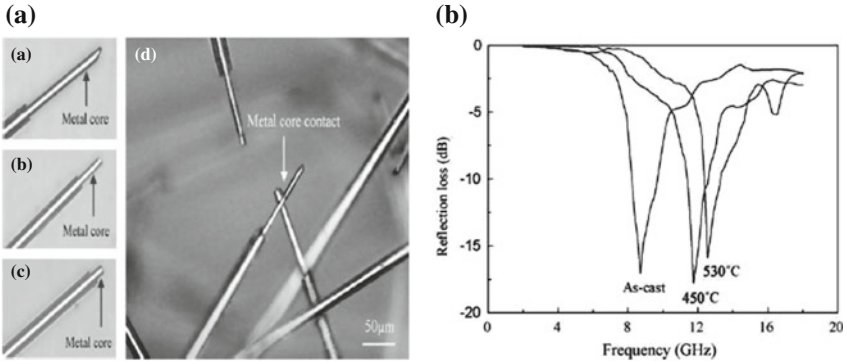

Fig. 12.3 **a** Morphology and metal core contact of the short-cut microwires: (*a*) as-cast; (*b*) annealed at 450 °C; (*c*) annealed at 530 °C; (*d*) metal core contact (as-cast). **b** Calculated reflection losses of planar composites filled with as-cast and annealed microwires (with filling ratio of 15 % and thickness of 1.5 mm). Reprinted with the permission from [2], copyright 2010 Elsevier

the microwave absorption. Indeed, it is shown that the percolation threshold decreases due to the decrease of the length of the naked metallic core via annealing, but the level of maximum absorption is retained. It can then be expected that with a further increase of the annealed wire concentration, the absorption can be increased.

Among the dilute absorbers, the one proposed by Liu et al. [26] is unique as it was made transparent by dispersing short-cut microwires of lengths from 5 to 12 mm into a transparent siliconeelastomer. Such a transparent microwire composite shows more than 10 dB of shielding efficiency with just 0.5 wt% microwires and a thickness of less than 750 μm. The study reveals that a wire length of around 10 mm (with a tolerance of less than 0.4 mm) is the optimum parameter for shielding purposes. The shielding profiles are determined by the wire resonance, depending on the wire length and cluster effect [27].

Qin et al. [7, 28] conducted a detailed study on the influence of the wire diameter, interwire spacing, and the embedded depth on the absorption performance in a set of E-glass fibre-reinforced polymer (GFRP)/microwire composites. They used an equivalent circuit model as shown in Fig. 12.4 to illustrate the influence of these geometrical parameters. Figure 12.5a shows that in the continuous-wire composite with fixed interwire spacing b, reducing b will effectively increase absorption, which can be explained by an equivalent circuit. When an array of microwires is excited by a microwave with electric field e polarised along the microwire, the displacement current flows along both the microwires and the air gaps between neighbouring wires. Hence, the system can be regarded as a parallel combination of lumped impedances; the impedances of the wire and air gap are formulated as follows:

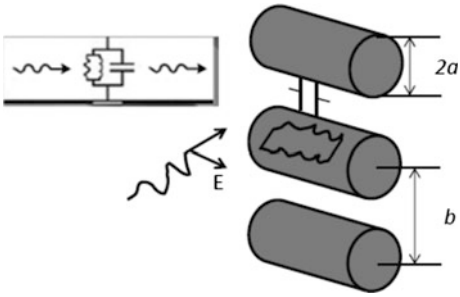

Fig. 12.4 Schematic of equivalent circuit for array of wires excited by an incident microwave with the electrical field component along the wire axes *a* and *b* denote the wire radius and interwire spacing, respectively

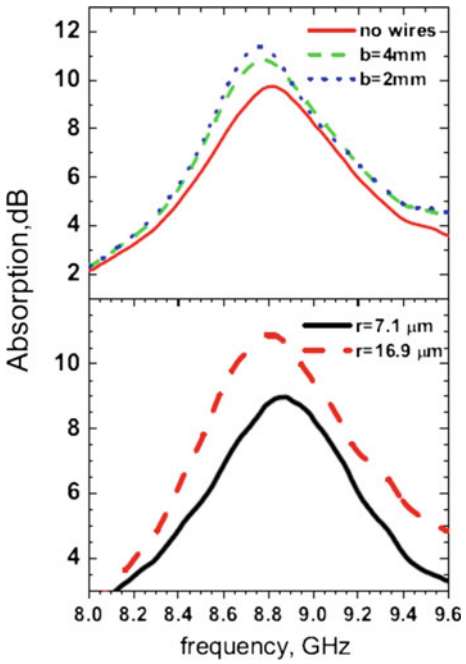

Fig. 12.5 **a** Absorption spectra for continuous microwire/GFRP composites with different wire spacing *b*. **b** Absorption spectra for continuous microwire/GFRP composites with wires of different radius *a*. Reprinted with the permission from [28], copyright 2013 Springer

$$Z_{\text{wire}} = i/\omega\pi a^2\varepsilon_{\text{wire}}; \tag{12.24a}$$

$$Z_{\text{air}} = \frac{i}{\omega(2rb - \pi a^2)\varepsilon_{\text{air}}}, \tag{12.24b}$$

where $\varepsilon_{\text{wire}}$ and ε_{air} are the permittivities of the studied microwire and air gaps; ω is the angle frequency; *a* denotes the radius of the wire. The equivalent impedance $Z_{\text{eq-wire}}$ of the wire/gap system can then be given by

$$Z_{\mathrm{eq-wire}} = \frac{Z_{\mathrm{wire}} Z_{\mathrm{air}}}{Z_{\mathrm{wire}} + Z_{\mathrm{air}}}. \tag{12.25}$$

With reference to the above equations, $Z_{\mathrm{eq-wire}}$ is improved with decreasing b, and consequently reduces transmission and increases absorption. Some comments are in order here. (i) By varying the equivalent impedance of the circuit, the absorption (or transmission) spectra can be modulated; this is very useful for developing effective filters. (ii) By selecting different b and r, one can formulate and control the change of the absorption maximum and the shift of absorption, which can be exploited for metamaterial applications. This effect is exemplified in Fig. 12.5a: as b is reduced, the absorption maximum redshifts and the absorption bandwidth are broadened. This is consistent with the theoretical calculations in [29], which reports that a metal-backed quarter-wavelength radio-absorber containing an array of ultrathin microwires of 4 μm radius exhibits improved absorption and redshift of the absorption peak as the wire spacing is reduced from 10 mm to 1 mm. It should be noted that maximising the function of one parameter that constitutes the mesostructure of composites for modulating the microwave properties also relies on the optimisation of other pertinent parameters [30].

This may explain why the shift presented for the current case is not significant. Indeed, the best absorption performance should meet impedance matching conditions that can only be achieved with appropriate wire impedance, diameter, and spacing [29]. It is expected that further reduction of the airgap (wire spacing) will raise absorption; but when the wires spacing is reduced to be small enough to induce indirect dipolar interactions or even direct exchange interactions, the absorption mechanism will change from the domination of dielectric loss to that of magnetic loss [31] and the composite may become very lossy, while the maximum absorption will shift to a much higher frequency. It should be noted that the influence of interwire spacing on the microwave properties varies for different compositions of microwires. For composites containing continuous Co-based microwires, the dielectric response is sensitive to the external magnetic field via the strong magnetoimpedance effect [32]; but there is a lack of strong microwire interactions between the neighbouring wires and it is generally not possible to observe multiple resonances in the absorption spectra, even with very small spacing. In contrast, for the composites containing continuous Fe-based wires, the field effect is weak as the MI properties of Fe-based wires are inferior [33]; but with decreasing interwire spacing, the closing domain structure can be formed and the strong exchange resonance effect may be expected to benefit the absorption performance [34]. In either case, the wire spacing plays an important role in manipulating the electromagnetic behaviours.

In addition to the wire spacing, another equally important parameter is the wire diameter. As shown in Fig. 12.5b, although composites containing the same loading of thin wires have smaller wire spacing, larger absorption is observed in composites with a larger diameter than in those with smaller diameters. This can be understood

by a theoretical model for the effective permittivity ε_{eff} of wire arrays consisting of thin wires with diameters less than 40 μm [35]:

$$\varepsilon_{\text{eff}} = \varepsilon_0 - \frac{1}{\omega t b} \cdot \left(\frac{\omega L + X_{\text{W}}}{R_{\text{W}}^2} + j \frac{1}{R_{\text{W}}} \right), \tag{12.26}$$

where R_{W}, L, and X_{W} represent the dc resistance, inductance, and reactance of the wire, respectively. In this instance, the effective permittivity is determined by the wire resistance. Thicker wire has smaller resistance and hence larger permittivity; its composite therefore shows better absorption. In addition, although the ratio of the radius square to the wire spacing remains the same for the two composites with the same loading of wires, the composite with thicker wire experiences a stronger skin effect and reduces the value of matching spacing, thereby achieving better impedance matching than with thinner wires in this case [29]. It should be noted that as the wire gets thicker than 40 μm, the inverse relation between ε_{eff} and R_{W} switches to proportional; this was demonstrated in the preceding chapter. This is reasonable as, although the good conductivity of absorbents is essential for absorption, too high conductivity will make the material excessively reflective. On this basis, the above argument is valid that larger permittivity results in larger absorption, as the permittivity here is circumstanced by polarisation only, excluding conduction. In another perspective, embedding a too thick wire into the polymer matrix will lead to a significant diameter mismatch compared with typical reinforcing fibres of 8–12 μm [36], thereby degrading the mechanical properties of the resulting composites. As such, limitation of the wire diameter can retain the advantages of the lightweight structure intrinsic to polymer composites and is thus preferable for the overall composite performance. This consideration should be adopted as a strategy to design multifunctional composites enabled by these Fe-based microwires.

Further study has been conducted upon the effect of embedded depth (the distance of the ferromagnetic microwire layer to the microwave incident surface) on the resultant absorption performance by the same group. They examined whether wires put in the front or back have different responses; indeed, the back-wire sample shows better absorption due to the contribution of the front GFR player and the back wire layer. The even-poorer absorption than the pure GFRP with the wires in the front layer as observed is attributed to the reflection induced by the wires. This clearly suggests that the wires should not be embedded in the front layer so as to prevent a significant impedance mismatch in the surface layer that reflects the wave away. They also tested the configuration with wires embedded in the medium layer, as shown in Fig. 12.6a. The results show that they did not present as good absorption. The second layer of GFRP serves as a substrate layer to slightly increase the impedance mismatch [37], so the absorption is slightly decreased and also the matching frequency is shifted as compared to the single layer, but it is similar to the first configuration, which further substantiates the function of the GFRP as the substrate layer. The fourth configuration shows greatly decreased absorption, which is due to the reflection of the GFRP; this is further confirmed by the case of

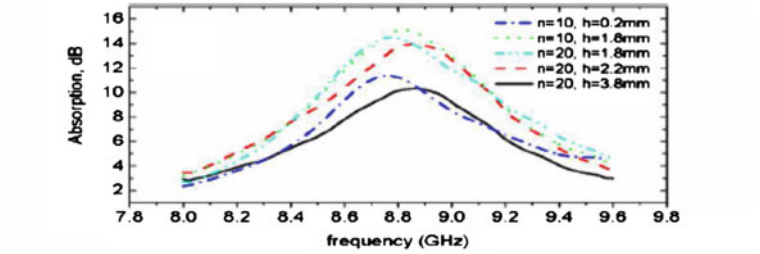

Depth	0.2 mm	1.8 mm	1.8 mm	2.2mm	3.8mm
Configuration					
Absorption (dB)	11.5268	15.6268	14.6284	14.3997	10.5430
Frequency(GHz)	8.7680	8.8260	8.7860	8.8260	8.8260

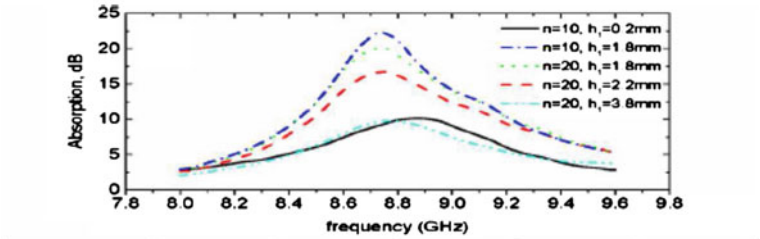

h_1	0.2 mm	1.8 mm	1.8 mm	2.2 mm	3.8 mm
h_2	0.4 mm	1.6 mm	1.6 mm	2.4 mm	3.6 mm
Configuration					
Absorption (dB)	9.9599	22.7887	20.6091	17.0009	10.2595
Frequency(GHz)	8.7860	8.7300	8.7120	8.7200	8.9140

Fig. 12.6 **a** Influence of embedded depth h_i of the ith microwire layer on the absorption spectra for continuous microwire/GFRP composites with 0° wire orientation. The values of h_1 and n (number of laminates) are indicated in the figure legend; the maximum absorption for each composite configuration is summarised in the table below. **b** Same as **a** but with the addition of another layer (h_2) of microwires. Reprinted with the permission from [28], copyright 2013 Springer

3.8 mm embedded depth. The composites containing two layers of microwires of the same configuration are also examined. With reference to Fig. 12.6b, the addition of a second layer of wires retains the same sequence of configuration ranked in terms of absorption, except for the first configuration, i.e. wires at the top with respect to the incident wave, whereby the absorption is the least of all due to very strong reflection. Similar results have been reported for the case of the absorber containing 1-mm microwire absorbents [38], whereby the best absorption has been achieved when the wires are positioned close to the metallic substrate.

The importance of the above result lies in the simultaneous achievement of the optimal absorption and the impact resistance performance offered by the same configuration of such microwire/GFRP composites. GFRPs are widely used in wind turbines, which are essential structural components for wind energy harvesting. As wind turbines can cause interference to normal radar communications due to the unwanted Doppler returns [39], the introduction of wires into GFRP will mitigate the issue and address this conflict of interest between the desire to encourage wide use of renewable and green energy and the desire to maintain the effective operation of the important human safety-associated radars used for air traffic control, weather monitoring, and marine navigation aids.

12.3 Magnetic Loss Dominated Absorbing

In the case of microwire composites with heavy loading, the ferromagnetic resonance may shift to gigahertz frequency due to the enhanced effective anisotropy field via the long-range dipolar interactions between wires [3, 40]. In this case, the ferromagnetic resonance for the planar microwire composites is given by [40]

$$f_{\mathrm{r}} = r\sqrt{4\pi M_{\mathrm{s}}(H_{\mathrm{k}} + H_{\mathrm{n}})}; \tag{12.27a}$$

$$H_{\mathrm{n}} \propto iM_{\mathrm{s}}(a/l)^2, \tag{12.27b}$$

where H_{n} is the field created by neighbouring wires of total number i, or it can be simply understood as an additional anisotropy field induced by wire interactions [41]. Thus, any factors that can influence the anisotropy field should be considered tuning parameters. Directly from Eqs. 12.27a and 12.27b, it is obtained that a larger aspect ratio ($l/2a$) will reduce the resonance frequency and increase the absorption according to Snoek's law; and that the increasing number of wires will enhance the permeability and neighbouring field and hence the resonance frequency. For Co-based wires, the decrease of metal-to-total diameter ratio p will elevate the internal stress and consequently the anisotropy field [42, 43], thus the absorption should be shifted to a higher frequency. This has been analytically explained very well by Baranov et al. [44]. The dependence of resonance frequency can be expressed as follows:

$$f \approx f_0\sqrt{\left(\frac{1-p^2}{1+1.5p^2}\right)}\ (\mathrm{GHz}), \tag{12.28}$$

where

$$f_0 = 1.5\sqrt{\lambda \times 10^6}\ (\mathrm{GHz}). \tag{12.29}$$

Also, note that the reduction of the wire core diameter can reduce the thickness of the outer shell of the domain so that the electromagnetic wave can penetrate into the inner core with an axial anisotropy and easily induce natural ferromagnetic resonance. As the reduced wire diameter can also guarantee a lightweight structure, it is therefore desirable to use very fine wires of less than 20 μm diameter to make absorbers.

Three kinds of microwires of typical positive, negative, and vanishing magnetostriction constant with correspondingly different composition [45] are chosen here to shed light on the usefulness of this theory. By using Eq. (12.28), the metal-to-total diameter (p) dependence of the resonance frequency is calculated for these three wires. The result confirms the role of the wire's cross-sectional geometry on the natural ferromagnetic resonance frequency and also reveals that the Fe-based wires are more suitable for absorption purposes at relatively higher gigahertz frequencies. This is consistent with three ported magnetoabsorption properties of wires with positive, negative, and vanishing magnetostriction constant [46]. For microwave absorption purposes, the best configuration, with respect to the wire axis, is when the static magnetic field and the microwave electrical field are parallel; the microwave magnetic field is perpendicular, as in such configuration, and circumferential FMR will be induced with marked intensity by the microwave electrical field [47]. In contrast, the ferromagnetic resonance induced by the magnetic component of the microwave is much weaker in microwires and can only be well observed in the submicron wires and nanowires [48]. Such a remarkable dependence of FMR on the wire orientation with respect to the microwave and external magnetic field has been well studied in [46]. As shown in Fig. 12.7, we can deduce that, under a constant magnetic field, tilted wires with respect to the axis will give much smaller absorption intensity, and that when the angle increases to a certain value (approaching 90°), the FMR will disappear unless a much higher magnetic field is applied. Also, one can see that the Fe-based wires are the best option for

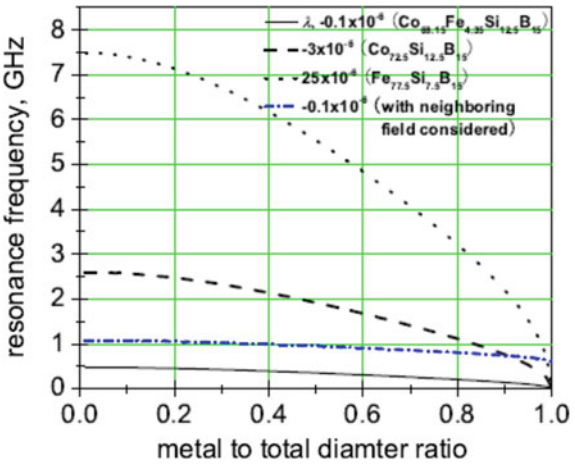

Fig. 12.7 Dependence of resonance field (H_{res}) of absorption spectra on the microwire orientation (α) with respect to the static magnetic field as shown in the inset at 9.5 GHz. Reprinted with the permission from [46], copyright 2002 Elsevier

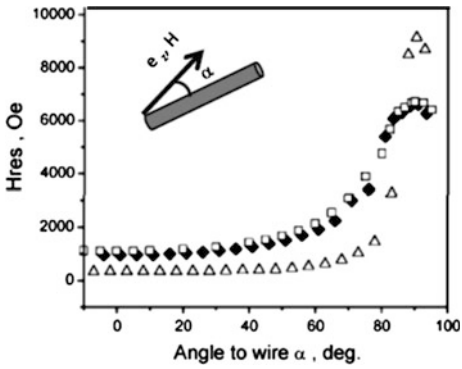

Fig. 12.8 Theoretical curve (*continuous line*) of FMR frequency as a function of x according to Eq. 12.28 for three wires with positive, negative, and vanishing magnetostriction, respectively

magnetic microwires, since they have the largest tolerance to the tilted angle range up to 80° without significant increase of the resonance magnetic field. Clearly this suggests that, for a quasi-isotropic magnetic absorber with wires homogeneously dispersed, Fe-based microwires are more efficient than other types of wires since the effective amount of Fe-based wires, regardless of the orientation of the EM wave, will be larger than other kinds of wires.

Another feature of great interest is that the resonance frequency can be shifted to higher frequency if a large enough neighbouring field is yielded with a good number of wires added into the absorbing medium or tailored wire geometry (Fig. 12.8). A proven method is to make a multilayer-structured microwire film that will enhance the anisotropy field [49] and give an improved initial permeability, as high as 6000 at 1 MHz. With the reduction of the wire length, the demagnetising field increases, and the anisotropy field is reduced accordingly [3, 5, 41, 50], resulting in the reduction of absorption via the collaborative effect with the influence on the neighbouring field H_n. In general, the optimal dimensions for excellent absorption performance require a metallic core of diameter 1–3 μm and length 1–3 mm, comparable to the half wavelength [51] for microwires.

Several important aspects of the implementation of microwires on absorbers should be highlighted here. First, as the anisotropy constant of microwires can be conveniently modulated by the magnetostriction constant, which is subject to the wire composition and stress conditions (either internal stress from different geometry or external stress applied), the tuning of natural FMR resonance and associated absorption features such as the absorption maximum and bandwidth is therefore readily accessible. Second, the dispersion of microwires (i.e. mesostructure control) is critical to meet the requirement for suitable dimensions [51] and arrangements for maximum absorption. As discussed above, the dispersion can have an impact on the orientation of wires and hence the electromagnetic absorption behaviour. This partially explains why the theoretical calculation from complex permittivity and permeability that is obtained typically in a wax-based toroidal

sample usually does not match the reflection loss experimentally measured with planar samples of much larger size (e.g. [2]). Tunable absorption can be realised in the absence of magnetic field and prefers an ultrathin metallic core, making the wires attractive for miniaturisation of microwave devices based on these fine elements. The last important aspect meriting our attention is the use of wires without glass coatings. Although they are inferior in terms of as-cast wire quality due to the fabrication limitation as compared to glass-coated wires, it is the metallic core rather than the glass coating that interacts effectively with the microwave. As such, applying the metallic core only into the absorbing matrix will improve the packing density of the wires [49] and hence the absorbing rate and efficiency. However, an obvious drawback requiring caution is that they can form a percolation network at certain concentrations and will thus induce large reflection. Such a percolating effect explains why weak permittivity is observed for 80 wt% melt-extracted FeSiB wires in a toroidal sample as reported in [52]. The absorption thus calculated is of little practical interest, with over 10 dB loss only occurred at 1–2.7 GHz for thicknesses over 4 mm. This performance is much inferior to what Marin et al. [4] have presented with wires of similar static magnetic behaviour, i.e. more than 15 dB at 8.5 GHz with a wire fraction of *c.a.* 3.1wt%.

12.4 Other Absorbers Based on Microwires

In this section, we will discuss some strategies for designing specific absorbers with microwires or microwire-based absorbents based on the limited data reported in the literature. One approach is to use hybrid microwires with dielectric absorbents or to design a (gradient) multilayer structure to improve the impedance mismatch and hence improve the absorption. The other is to fabricate multilayer microwires by coating with additional layer(s) of magnetic and/or non-magnetic phases so as to yield additional absorption peaks.

Qin et al. [53] propose hybridising microwires with carbon nanotubes (CNT) with good electrical conductivity to make a multiscale hybrid composite absorber. As shown in a group of spectra of lossy parameters (Fig. 12.9), the loss tangent increases significantly with increasing wire concentration, suggesting the possibility of improved absorption; while the intrinsic impedance calculated from $\eta = \sqrt{\mu/\epsilon}$ shows an opposite trend, which is due to the increased conduction loss, although the polarisation loss is also improved. Indeed, the reflection is increased. One can also see that the absorption has been enhanced with the co-work of the wires and CNTs.

Torrejon et al. [54] developed a biphase magnetic microwire consisting of a soft amorphous nucleus and harder outer crystalline shell. The presence of additional hard phase as compared to the conventional single-phase microwire induces a second absorption peak at a lower frequency than that excited in the soft nucleus. Although the second peak is weaker, it helps generate an additional absorption peak and hence enlarge the absorption band. However, a serious issue with this kind of

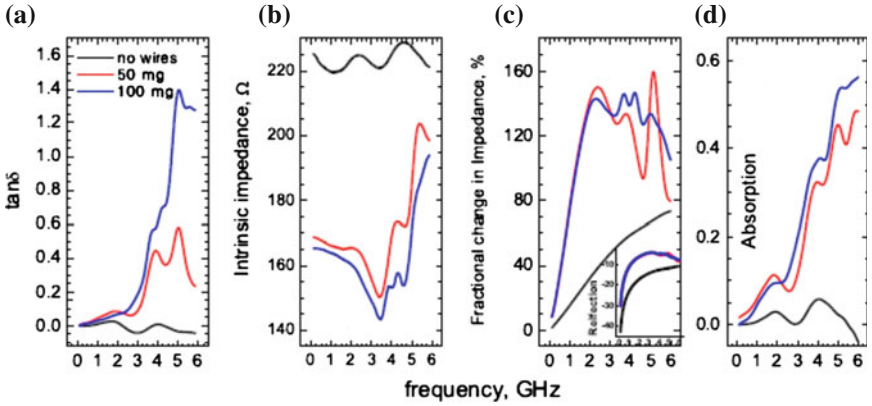

Fig. 12.9 Frequency dependences of loss tangent (**a**), intrinsic impedance (**b**), fractional change in surface impedance (**c**), and absorption (**d**). Reprinted with the permission from [53], copyright 2013 Elsevier

multilayer wire is the tremendous reduction of the magnetoabsorption level compared with conventional glass-coated wires, which is suggested to be attributable to the reduced volume fraction of the inner axial domain in the amorphous nucleus caused by the electroplating-induced stresses. A proper post-annealing is apparently necessary to resolve this problem.

In closing, with all the advantages discussed above at VHF frequency, the microwires can be effectively designed in terms of composition, static magnetic properties, geometry (core diameter, metal-to-total diameter ratio, length, and aspect ratio), concentration, topological arrangement (unidirectional and omni-directional) with the guide of transmission-line theory and when fabricated by a facile mould-casting technique, yielding exceptional absorption or shielding performance. The absorption is readily tunable to meet frequency selective applications. Undoubtedly, the microwire composites can find a market niche as high-performance absorbers for anechoic chambers, modern concealment, biological protection shelters, and so forth.

References

1. Vazquez M, Adenot-Engelvin AL (2009) Glass-coated amorphous ferromagnetic microwires atmicrowavefrequencies. J Magn Magn Mater 321:2066–2073
2. Zhang Z, Wang C, Zhang Y, Xie J (2010) Microwave absorbing properties of composites filled withglass-coated $Fe_{69}Co_{10}Si_8B_{13}$ amorphous microwire. Mater Sci Eng 175:233–237
3. Di Y, Jiang J, Du G, Tian B, Bie S, He H (2007) Magnetic and microwave properties of glass-coated amorphous ferromagnetic microwires. Trans Nonferrous Met Soc China 17:1352–1357

4. Marin P, Cortina D, Hernando A (2005) High-frequency behavior of amorphous microwires and its applications. J Magn Magn Mater 290–291:1597–1600
5. Qin F, Peng H, Pankratov N, Phan M, Panina L, Ipatov M, Zhukova V, Zhukov A, Gonzalez J (2010) Exceptional EMI shielding properties of ferromagnetic microwires enabled polymer composites. J Appl Phys 108:044510
6. Skarman B, Ye Z, Jansson P (2011) Soft magnetic composite materials. US Patent 8,075,710
7. Qin F, Peng H, Chen Z, Hilton G (2013) Microwave absorption of structural polymer composites containing glass-coated amorphous microwires. IEEE Trans Magn 49:4245–4248
8. Liu L, Rozanov K, Abshinova M (2013) Tunable properties of microwire composites at microwavefrequency. Appl Phys A 110:275–279
9. Ababei G, Chiriac H, David V, Dafinescu V, Nica I (2013) Omni-directional selective shielding material based on amorphous glass coated microwires. Rev Sci Instrum 83:014701–014706
10. Liberal I, Ederra I, Gomez-Polo C, Labrador A, Perez-Landazabal JI, Gonzalo R (2011) Theoretical modeling and experimental verification of the scattering from a ferromagnetic microwire. IEEE Trans Microwave Theor Tech 59:517–526
11. Dawson TW, Caputa K, Stuchly MA, Shepard RB, Kavet R, Sastre A (2002) Pacemaker interferenceby magnetic fields at power line frequencies. IEEE Trans Biomed Eng 49:254–262
12. Colin R (1966) Foundations of mIcrowave engineering. McGraw Hill, New York
13. Vinoy KJ, Jha RM (1996) Radar absorbing materials - From theory to design and characterization. Kluwer Academic Publishers, Boston
14. Oh JH, Oh KS, Kim CG, Hong CS (2004) Design of radar absorbing structures using glass/epoxy composite containing carbon black in x-band frequency ranges. Compos B Eng 35:49–56
15. Shen G, Xu Z, Li Y (2006) Absorbing properties and structural design of microwave absorbers based on w-type la-doped ferrite and carbon fiber composites. J Magn Magn Mater 301:325–330
16. Gerber R, Wright C (eds) (1992) GA. Applied magnetism. Kluwer Academic Publishers, Doldrecht
17. Kittel C (1948) On the theory of ferromagnetic resonance absorption. Phys Rev 73:155
18. Maeda T, Sugimoto S, Kagotani T, Tezuka N, Inomata K (2004) Effect of the soft/hard exchangeinteraction on natural resonance frequency and electromagnetic wave absorption of the rareearth-iron-boron compounds. J Magn Magn Mater 281:195–205
19. Acher O, Dubourg S (2008) Generalization of snoek's law to ferromagnetic films and composites. Phys Rev B 77:104440
20. Makhnovskiy DP, Panina LV (2005) Field and stress tunable microwave composite materials based on ferromagnetic wires. In: Murray VN (2005) Progress in ferromagnetism research. Nova Science Publishers Inc., Hauppauge
21. Starostenko S, Rozanov K, Osipov A (2006) Microwave properties of composites with glass coated amorphous magnetic microwires. J Magn Magn Mater 298:5–64
22. Fan ZJ, Luo GH, Zhang ZF, Zhou L, Wei F (2006) Electromagnetic and microwave absorbing properties of multi-walled carbon nanotubes/polymer composites. Mater Sci Eng B-Solid State Mater Adv Technol 132:85–89
23. Liu ZF, Bai G, Huang Y, Li FF, Ma YF, Guo TY, He XB, Lin X, Gao HJ, Chen YS (2007) Microwave absorption of single-walled carbon nanotubes/soluble cross-linked polyurethane composites. J Phys Chem C 111:13696–13700
24. Wu KH, Ting TH, Wang GP, Ho WD, Shih CC (2008) Effect of carbon black content on electrical and microwave absorbing properties of polyaniline/carbon black nanocomposites. PolymerDegrad Stability 93:483–488
25. Baranov SA (1998) Use of a microconductor with natural ferromagnetic resonance for radio absorbing materials. Tech Phys Lett 24:21–23
26. Liu L, Yang Z, Kong L, Li P, Poo C (2012) High permittivity and shielding effectiveness of microwire composites with optical transparency. In: 2012 Asia-Pacific symposium on electromagnetic compatibility (APEMC). IEEE, pp 633–636

27. Liu L, Matitsine S, Gan YB, Rozanov KN (2007) Cluster effect in frequency selective composites with randomly distributed long conductive fibres. J Phys D Appl Phys 40:7534
28. Qin F, Peng H, Chen Z, Wang H, Zhang J, Hilton G (2013) Optimization of microwire/glass-fiber reinforced polymer composites for wind turbine application. Appl Phys A Mater Sci Process. 10.1007/s00339-013-7820-2
29. Ponomarenko V, Popov V, Qin F (2013) Microwire-based analog of a quarter-wavelength radio absorber. Radio Electron Commun Syst 56:285–289
30. Brosseau C, Queffelec P, Talbot P (2001) Microwave characterization of filled polymers. J Appl Phys 89:4532–4540
31. Qin FX, Peng HX (2013) Ferromagnetic microwires enabled multifunctional composite materials. Prog Mater Sci 58:183–259
32. Qin FX, Peng HX, Phan MH, Panina LV, Ipatov M, Zhukov A (2012) Effects of wire properties on the field-tunable behaviour of continuous-microwire composites. Sens Actuators A 178:118–125
33. Phan MH, Peng HX (2008) Giant magneto impedance materials: fundamentals and applications. Prog Mater Sci 53:323–420
34. Chizhik A, Zhukov A, Blanco JM, Szymczak R, Gonzalez J (2002) Interaction between Fe-richferromagnetic glass-coated microwires. J Magn Magn Mater 249:99–103
35. Liberal I, Nefedov I, Ederra I, Gonzalo R, Tretyakov S (2011) Electromagnetic response and homogenization of grids of ferromagnetic microwires. J Appl Phys 110:064909
36. Qin F, Peng HX, Tang J, Qin LC (2010) Ferromagnetic microwires enabled polymer composites for sensing applications. Compos A Appl Sci Manuf 41:1823–1828
37. Qin F, Brosseau C (2012) A review and analysis of microwave absorption in polymer composites filled with carbonaceous particles. J Appl Phys 111:061301–061324
38. Marin P, Cortina D, Hernando A (2008) Electromagnetic wave absorbing material based on magnetic microwires. IEEE Trans Magn 44:3934–3937
39. Krug F, Lewke B (2009) Electromagnetic interference on large wind turbines. Energies 2:1118–1129
40. Ivanov AV, Shalygin AN, Galkin VY, Vedyayev AV (2009) Rozanov3 KN. Meta materials with tunable negative refractive index fabricated from amorphous ferromagnetic microwires: magneto static interaction between microwires. PIERS ONLINE 5:649–652
41. Di Y, Jiang J, Bie S, Yuan L, Davies HA, He H (2008) Collective length effect on the magneto static properties of arrays of glass-coated amorphous alloy microwires. J Magn Magn Mater 320:534–539
42. Zhukov A, Zhukova V (2009) Magnetic properties and applications of ferromagnetic mircowires with amorphous and nano crystalline structure. Nova Science Publishers, Inc., New York
43. Usov N, Antonov A, Dykhne A, Lagar'kov A (1998) Stress dependence of the hysteresis loops ofco-rich amorphous wire. J Phys: Condens Matter 10:2453
44. Baranov S (2009) Radio absorption properties of amorphous microwires. Moldavian J Phys Sci 8:332–336
45. Garcia D, Raposo V, Montero O, Iniguez JI (2006) Influence of magnetostriction constant on magneto impedance-frequency dependence. Sens Actuators A 129:227–230
46. Yildiz F, Rameev BZ, Tarapov SI, Tagirov LR, Aktas B (2002) High-frequency magneto resonance absorption in amorphous magnetic microwires. J Magn Magn Mater 247:222–229
47. Tulin V, Astahov M, Rodin A (2003) Amorphous ferromagnetic microwire in the microwave cavity. Ferromagnetic resonance and absorption. J Magn Magn Mater 258(C259):201 – 203 (Second Moscow international symposium on magnetism)
48. Kraus L, Infante G, Frait Z, Vazquez M (2011) Ferromagnetic resonance in microwires and nanowires. Phys Rev B 83:174438
49. Baranov S, Yamaguchi M, Garcia K, Vazquez M (2010) Application of amorphous microwires for electromagnetic shieldi. Moldavian J Phys Sci 9:76–82
50. Zhukova V, Usov NA, Zhukov A, Gonzalez J (2002) Length effect in a co-rich amorphous wire. Phys Rev B 65:134407

51. Baranov SA, Yamaguchi M, Garcia KL, Vazquez M (2008) Dimensional absorption high-frequency properties of the cast glass coated microwires. Surf Eng Appl Electrochem 44:425–427
52. Han M, Liang D, Deng L (2011) Fabrication and electromagnetic wave absorption properties of amorphousfe[sub 79]si[sub 16]b[sub 5]microwires. Appl Phys Lett 99:082503
53. Qin FX, Brosseau C, Peng HX (2013) Microwave properties of carbon nanotube/microwire/rubbermultiscale hybrid composites. Chem Phys Lett 579:40–44
54. Torrejon J, Badini-Confalonieri GA, Vazquez M (2009) Double-absorption ferromagnetic resonance in biphase magnetic microwires. J Appl Phys 106:023913